Five-Axis High Speed Machining of Sculptured Surfaces by Surface-Based NURBS Path Interpolation

John C. J. Chiou[1] and Yuan-Shin Lee[2]

[1]Unigraphics Solution, chiou@ugs.com
[2] North Carolina State University, yslee@ncsu.edu

ABSTRACT

This paper presents a new surface-based NURBS path interpolation for 5-axis high speed machining (HSM) of sculptured surfaces. Detailed formulation of the new time-parameter NURBS path interpolation is proposed to convert the NURBS part surface into time-variable parameterized tool paths for 5-axis sculptured surface machining. Based on the machine configurations, the surface-based NURBS path interpolation directly derives the pivot point location and the spindle orientation to control the machine motion. With the proposed new method, the traditional chordal and linearization deviation errors in 5-axis NC machining can be reduced. Computer implementations and illustrative examples are also presented in this paper. The presented techniques can be used in the CAD/CAM systems and the NC controllers for 5-axis high speed machining of sculptured surfaces.

Keywords: CAD/CAM/CNC, NURBS curve interpolation, Five-axis machining, Sculptured surfaces, High speed machining.

1. INTRODUCTION

High-Speed Machining (HSM) has become popular in both the research and the industry applications. HSM can improve the machining performance via the fast spindle rotation speed and feed-rate [1,2]. Feed-rate and acceleration control are critical issues to avoid the overshot and achieve good machining accuracy. New CNC machines have been developed to accept parametric curves for NC tool-path definition. Researchers have recently turned their interest into using parametric interpolation for high-speed machining of free-form surfaces. Compared with the traditional linear interpolation and circular interpolation, the parametric interpolation offers abundant advantages upon memory-size requirement, speed accuracy, position tracing error and jerk magnitude [3-6].

For sculptured surface machining, a free-form trajectory is traditionally approximated by a set of linear interpolations [7-9]. As shown in Fig 1, a linear approximation causes a chordal deviation when a free-form tool path is approximated by linear segments [10]. In addition, due to the combination of the translational and rotational movements, the actual cutter tip trajectory deviates from the linear segment (chord), which causes a swept deviation [11, 12]. As shown in Fig 1, the total machining errors in 5-axis machining consist of both swept deviation and chordal deviation. Using the linear interpolation methods, CAM systems have to generate a huge number of linear segments to approximate the free-form tool paths to achieve the required machining accuracy. Unfortunately, these short linear segments result in huge NC part programs, cause the unfavorable start-stop effects and prolong the total machining time [13].

To overcome such weaknesses, several curve interpolation methods were proposed [14-17]. The curve interpolators receive the parametric machine tool trajectories defined by only a small number of the control points in NC part programs. The machine tool trajectories are then generated to control the tool motions [18, 19]. This approach can bypass the time-consuming data downloading and generate smooth tool trajectories. However, the current CAM systems use lower degrees of curves to approximate the ideal machine tool trajectories [20]. As shown in Fig 2, the approximation curves only pass the given pivot points and they may not exactly match the ideal machine tool trajectories. An approximation error exists between the approximation curves and the ideal trajectories [21]. In addition, when the machining tolerance is tight, the approximation curves even require more data to represent the machine tool trajectories than the linear interpolation [20, 21].

To overcome the positioning error of the chordal deviations and the swept deviations and to make the NC part programs independent from the machine tool configurations, surface interpolations were proposed by several

researchers [1, 2, 16, 19]. The surface interpolations consist of tool path planning, inverse kinematics, and trajectory planning functions. The cutter location and orientation, in contrast to linear and curve interpolations, are not defined in NC codes. Instead, they are derived from the part surfaces and these part surfaces are defined in NC part programs. The surface interpolations have been successfully applied to 3-axis NC machining with ball-endmill, 5-axis ruled-surface machining and 5-axis convex-surface machining with flat-endmill. However, due to the surface interpolations lack of strategies in the tool path planning and gouge-interference prevention, the machining error problems may exist in the complex part geometry. Unfortunately, the part geometry in 5-axis NC machining is usually greatly complex.

In this paper, a new CAD/CAM/CNC manufacturing architecture and a new surface-based NURBS path interpolation is proposed for 5-axis machining of sculptured surfaces. The new architecture is shown in Fig 3. The machine inverse kinematics is performed in the interpolator, instead of traditionally in the post-processors. Details of the proposed method are discussed in the following section.

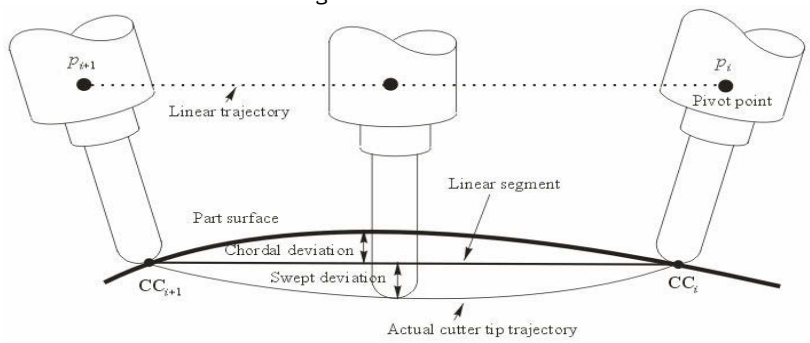

Fig. 1: Chordal deviation error and swept deviation error in 5-axis machining with linear interpolation.

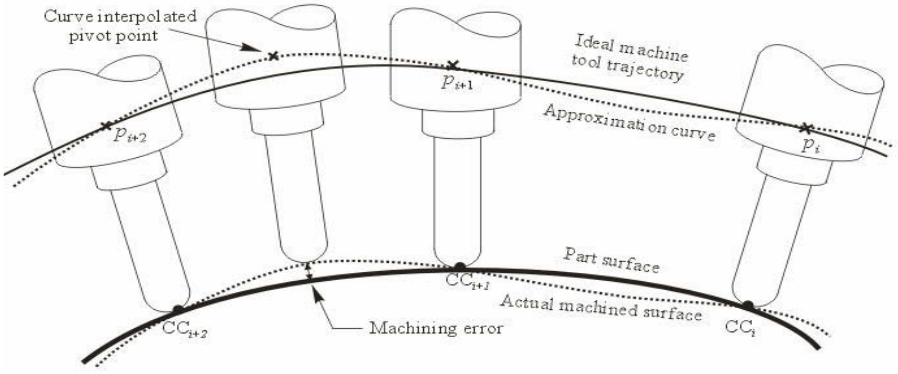

Fig. 2: Position errors in 5-axis machining with curve interpolation.

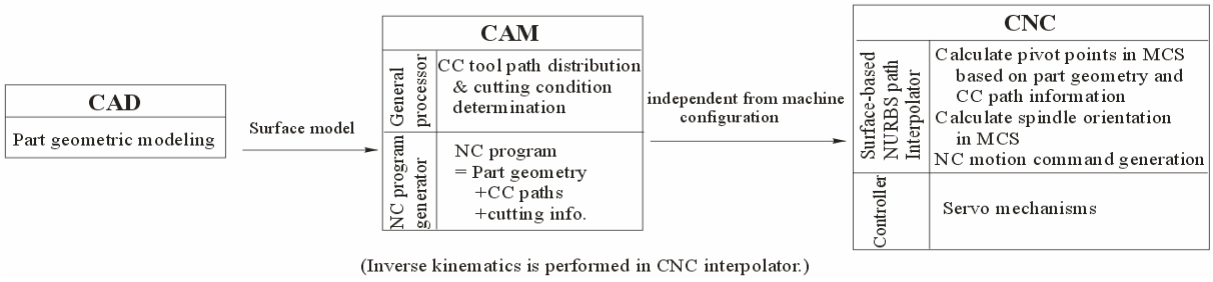

Fig. 3: Proposed CAD/CAM/CNC architecture.

2. BRIEF DISCUSSION OF NURBS CURVES AND SURFACES FORMULATION

To facilitate the detailed discussion of the proposed NURBS tool path interpolation, a brief discussion of the NURBS curves and surfaces is presented in this section. The NURBS (Non-Uniform Rational B-Splines) are the most commonly used parametric curve and surface representations in CAD/CAM/CNC systems [22, 23]. Here we briefly introduce the basic definitions and geometric properties of NURBS. A NURBS curve $C(\hat{w})$ is defined as follows [23]:

$$C = C(\hat{w}) = \frac{A_c(\hat{w})}{B_c(\hat{w})} = \frac{\sum_{i_c=0}^{n_c} N_{i_c,d_c}(\hat{w})\overline{W}_{i_c}P_{i_c}}{\sum_{i_c=0}^{n_c} N_{i_c,d_c}(\hat{w})\overline{W}_{i_c}}, \quad 0 \le \hat{w} \le 1 \tag{1}$$

where P_{i_c} represents the control points, $\overline{W}_{i_c}$ are the weights, and d_c is the degree of the curve. $N_{i_c,d_c}(\hat{w})$ is the non-rational B-spline basis function defined at the knot vectors [23]. From Eq (1), a generalized *k*th order derivative of a NURBS curve $C(\hat{w})$ can be formulated as follows [23]:

$$C^{(k)}(\hat{w}) = \frac{\partial^k C(\hat{w})}{\partial w^k} = \frac{A_c^{(k)}(\hat{w}) - \sum_{i=1}^{k}\binom{k}{i}B_c^{(i)}(\hat{w})C^{(k-i)}(\hat{w})}{B_c(\hat{w})} \tag{2}$$

Similar to the NURBS curves, a NURBS surface $S(u,v)$ in the 3D space can be defined as follows [23]:

$$S = S(u,v) = \begin{bmatrix} x(u,v) \\ y(u,v) \\ z(u,v) \end{bmatrix} = \frac{A(u,v)}{B(u,v)} = \frac{\sum_{i_n=0}^{n}\sum_{j_m=0}^{m} N_{i_n,d_u}(u)N_{j_m,d_v}(v)\overline{W}_{i_n,j_m}P_{i_n,j_m}}{\sum_{i_n=0}^{n}\sum_{j_m=0}^{m} N_{i_n,d_u}(u)N_{j_m,d_v}(v)\overline{W}_{i_n,j_m}}, \quad 0 \le u,v \le 1 \tag{3}$$

where d_u and d_v are the surface degrees of u and v parameters, respectively. P_{i_n,j_m} is the control points in the 3D space. $\overline{W}_{i_n,j_m}$ represents the corresponding weights of the control points. $N_{i_n,d_u}(u)$ and $N_{j_m,d_v}(v)$ are the non-rational B-spline basis functions defined at the knot vectors in *u* and *v* parameters. A (k^{th},l^{th}) order derivative of the NURBS surface $S(u,v)$ with respect to the parameter *u* and *v* can be determined as follows [23]:

$$S_{u^k v^l}^{(k,l)}(u,v) = \frac{\partial^{k+l} S(u,v)}{\partial u^k \partial v^l} = \frac{1}{B(u,v)}\left(A_{u^k v^l}^{(k,l)}(u,v) - \sum_{i=1}^{k}\binom{k}{i}B_{u^i v^0}^{(i,0)}(u,v)S_{u^{k-i}v^l}^{(k-i,l)}(u,v) - \sum_{j=1}^{l}\binom{l}{j}B_{u^0 v^j}^{(0,j)}(u,v)S_{u^k v^{l-j}}^{(k,l-j)}(u,v) - \sum_{i=1}^{k}\binom{k}{i}\sum_{j=1}^{l}\binom{l}{j}B_{u^i v^j}^{(i,j)}(u,v)S_{u^{k-i}v^{l-j}}^{(k-i,l-j)}(u,v)\right) \tag{4}$$

where $A_{u^k v^l}^{(k,l)}(u,v) = \sum_{i_n=0}^{n}\sum_{j_m=0}^{m}\frac{\partial^{(k,l)}\left(N_{i_n,d_u}(u)N_{j_m,d_v}(v)\right)}{\partial u^k \partial v^l}\overline{W}_{i_n,j_m}P_{i_n,j_m}$ and $B_{u^i v^j}^{(i,j)}(u,v) = \sum_{i_n=0}^{n}\sum_{j_m=0}^{m}\frac{\partial^{(i,j)}\left(N_{i_n,d_u}(u)N_{j_m,d_v}(v)\right)}{\partial u^i \partial v^j}\overline{W}_{i_n,j_m}$.

These formulations of NURBS curves and surfaces as well as their derivatives will be used later for the surface-based NURBS path interpolation.

3. ARBITRARY CUTTER CONTACT (CC) PATHS ON COMPLEX PART SURFACES

To machine a free-form surface along tool paths, we should first represent any tool paths on the surface [24]. Fig 4 shows an arbitrary curve $C_{xyz}(\hat{w})$ lying on a 3D (x-y-z) NURBS surface $S(u,v)$ and the curve's corresponding parameters (u_c,v_c) are represented in the 2D (*u*-*v*) parametric domain by a NURBS curve representation $C_{uv}(\hat{w})$. As shown in Fig 4, the 2D curve $C_{uv}(\hat{w})$ in the *u*-*v* domain can be defined by using Eq (1) with a continuous curve parameter $\hat{w}$ shown as follows:

$$C_{uv} = C_{uv}(\hat{w}) = \begin{bmatrix} u_c(\hat{w}) \\ v_c(\hat{w}) \end{bmatrix} = \frac{\sum_{i_{uv}=0}^{n_{uv}} N_{i_{uv},d_{uv}}(\hat{w})\overline{W}_{i_{uv}}P_{i_{uv}}}{\sum_{i_{uv}=0}^{n_{uv}} N_{i_{uv},d_{uv}}(\hat{w})\overline{W}_{i_{uv}}}, \quad 0 \le \hat{w} \le 1 \tag{5}$$

where $[u_c(\hat{w})\ v_c(\hat{w})]^T$ are the curve $C_{uv}(\hat{w})$ locations in the *u*-*v* domain, and $P_{i_{uv}}$ are the control points of $C_{uv}(\hat{w})$ in the *u*-*v* domain. For an arbitrary curve C_{xyz} lying on the NURBS surface $S(u,v)$ as shown in Fig 4, the C_{xyz} (in *x*-*y*-*z* space) can be defined by using Eq (3) with the parameters (u_c,v_c) defined in the *u*-*v* domain as follows [24]:

$$C_{xyz} = C_{xyz}(\hat{w}) = S(u_c(\hat{w}), v_c(\hat{w})) = \begin{bmatrix} x(u_c(\hat{w}), v_c(\hat{w})) \\ y(u_c(\hat{w}), v_c(\hat{w})) \\ z(u_c(\hat{w}), v_c(\hat{w})) \end{bmatrix} = \frac{\sum_{i_n=0}^{n}\sum_{j_m=0}^{m} N_{i_n,d_u}(u_c) N_{j_m,d_v}(v_c) \overline{W}_{i_n,j_m} P_{i_n,j_m}}{\sum_{i_n=0}^{n}\sum_{j_m=0}^{m} N_{i_n,d_u}(u_c) N_{j_m,d_v}(v_c) \overline{W}_{i_n,j_m}} \tag{6}$$

where $(u_c(\hat{w}), v_c(\hat{w}))$ are the corresponding curve parameters defined in the surface parametric *u-v* domain by Eq (5) [23]. For an arbitrary cutter contact (*CC*) curve C_{xyz} on a 3D (*x-y-z*) NURBS surface $S(u,v)$ as shown in Fig 4, C_{xyz} can be represented by Eq (6) with its corresponding parameters $(u_c(\hat{w}), v_c(\hat{w}))$ described by Eq (5).

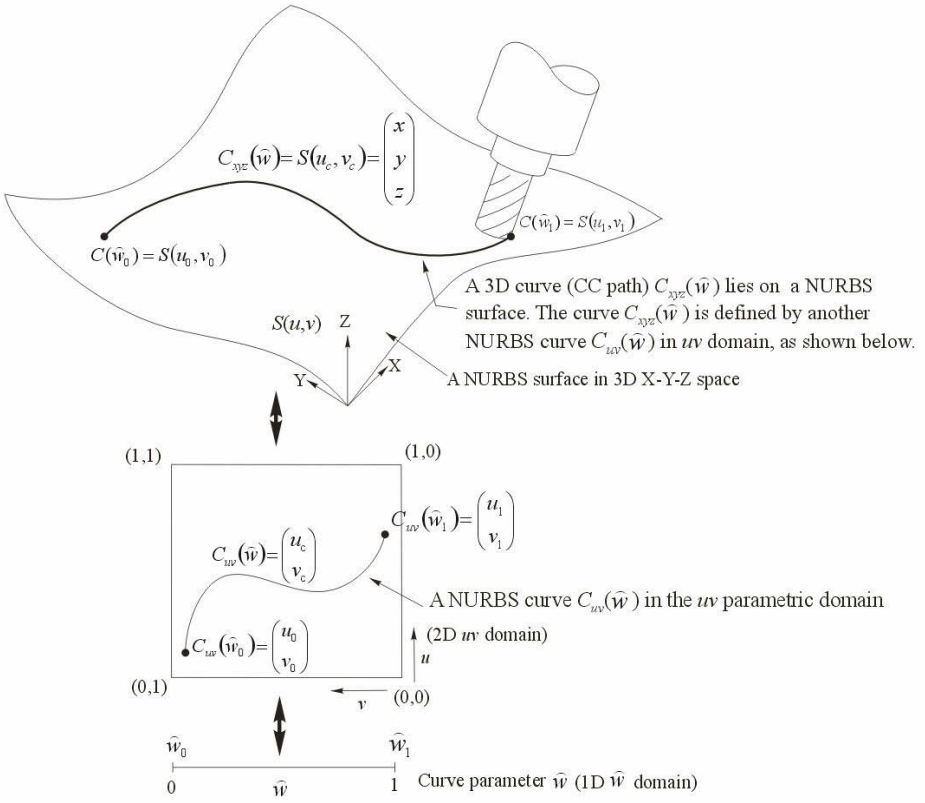

Fig. 4: Representing a 3D (X,Y,Z) curve in the 2D (u,v) domain and the 1D parameter (w) space.

4. VELOCITY ANALYSIS ALONG CUTTER CONTACT (CC) PATH

Besides presenting arbitrary tool paths on the sculptured part surface, feedrate control is also important during NC machining. When a cutter is moving along an arbitrary *CC* path $C_{xyz}(\hat{w})$ that lies on a NURBS part surface $S(u,v)$, the instantaneous speed vector $\vec{V}$ along the curve C_{xyz} can be defined by deriving Eq (6) with the time t as follows:

$$\vec{V} = \begin{bmatrix} V_x \\ V_y \\ V_z \end{bmatrix} = \dot{C}_{xyz} = \frac{dC_{xyz}}{dt} = \frac{\partial S}{\partial u}\frac{\partial u}{\partial \hat{w}}\frac{d\hat{w}}{dt} + \frac{\partial S}{\partial v}\frac{\partial v}{\partial \hat{w}}\frac{d\hat{w}}{dt} = \begin{bmatrix} \frac{\partial S}{\partial u} & \frac{\partial S}{\partial v} \end{bmatrix} \begin{bmatrix} \frac{\partial u}{\partial \hat{w}} \\ \frac{\partial v}{\partial \hat{w}} \end{bmatrix} \left(\frac{d\hat{w}}{dt}\right) \tag{7}$$

where *t* represents the time. $\partial S/\partial u$, $\partial S/\partial v$, $\partial u/\partial \hat{w}$, and $\partial v/\partial \hat{w}$ are defined by Eqs (2) and (4). To determine the motion speed $|\vec{V}|$ along an arbitrary *CC* path $C_{xyz}(\hat{w})$, we have

$$|\vec{V}|^2 = \dot{C}_{xyz}^2 = \dot{C}_{xyz}^T \dot{C}_{xyz} = U'^{\mathrm{T}} G U' \left(\frac{d\hat{w}}{dt}\right)^2 \tag{8}$$

where $U' = \begin{bmatrix} \frac{\partial u}{\partial \hat{w}} \\ \frac{\partial v}{\partial \hat{w}} \end{bmatrix}$, $G = \begin{bmatrix} \frac{\partial S}{\partial u} \cdot \frac{\partial S}{\partial u} & \frac{\partial S}{\partial u} \cdot \frac{\partial S}{\partial v} \\ \frac{\partial S}{\partial v} \cdot \frac{\partial S}{\partial u} & \frac{\partial S}{\partial v} \cdot \frac{\partial S}{\partial v} \end{bmatrix}$.

In Eq (8), G is the first fundamental matrix of the surface [25]. If we specify the motion speed $|\vec{V}|$ of a point moving along the arbitrary CC path $C_{xyz}(\hat{w})$ as a given speed $V_{\text{feedrate}}(\hat{w})$, we have

$$|\vec{V}| = \sqrt{U'^{T} G U'} \frac{d\hat{w}}{dt} = V_{\text{feedrate}}(\hat{w}) \tag{9}$$

where $V_{\text{feedrate}}(\hat{w})$ is a given motion speed (feedrate) of a cutter contact (CC) point moving along the arbitrary curve $C_{xyz}(\hat{w})$ during NC machining. From Eq (9), the relationship between the time t and the curve parameter $\hat{w}$ can be represented as follows:

$$\int_{\hat{w}_k}^{\hat{w}_{k+1}} d\hat{w} = \int_{t_k}^{t_{k+1}} \frac{V_{\text{feedrate}}(\hat{w})}{\sqrt{U'^{\mathrm{T}} G U'}} dt = \int_{t_k}^{t_{k+1}} \frac{\tilde{V}_{\text{feedrate}}(t)}{\sqrt{\tilde{U}'^{\mathrm{T}}(t) \tilde{G}(t) \tilde{U}'(t)}} dt \tag{10}$$

Note that during the tool motion control, the parameter $\hat{w}$ is a function of the time t. The $V_{\text{feedrate}}(\hat{w}) / \sqrt{U'^{\mathrm{T}} G U'}$ in Eq (10) can be transformed into a function of t, i.e., $\hat{w} = \hat{w}(t)$ and $\frac{V_{\text{feedrate}}(\hat{w})}{\sqrt{U'^{\mathrm{T}} G U'}} = \frac{\tilde{V}_{\text{feedrate}}(t)}{\sqrt{\tilde{U}'^{\mathrm{T}}(t) \tilde{G}(t) \tilde{U}'(t)}}$.

To maintain the pre-defined cutting feedrate $V_{\text{feedrate}}(\hat{w})$, the machine control unit needs to find the corresponding parametric increment $\Delta\hat{w}_k$ (where $\Delta\hat{w}_k = \hat{w}_{k+1} - \hat{w}_k$) to locate the next reference position at each sampling time ΔT ($\Delta T = t_{k+1} - t_k$). In Eq (10), the parameters $\hat{w}_k$, t_k, t_{k+1} and the feedrate $V_{\text{feedrate}}(\hat{w})$ are known ($\hat{w}_k$ is the current curve parameter, t_k is the current time, $t_{k+1} = t_k + \Delta T$ and $V_{\text{feedrate}}(\hat{w})$ is the given feedrate.). The parameter $\hat{w}_{k+1}$ can be found to determine the next reference position. Usually it is difficult to find $\hat{w}_{k+1}$ by directly solving Eq (10) with the known $\hat{w}_k$, t_k and t_{k+1}. However, when the sampling time period ΔT is small, we can use Taylor's expansion to approximate the function and to find the new curve parameter $\hat{w}_{k+1}$. From Eq (10), we have

$$\hat{w}_{k+1} = \hat{w}_k + \frac{d\hat{w}}{dt}(t_{k+1} - t_k) + \frac{d^2\hat{w}}{dt^2}(t_{k+1} - t_k)^2 + \varepsilon(\Delta T) \tag{11}$$

where $\varepsilon(\Delta T)$ is the error term, and $\varepsilon(\Delta T)$ becomes negligible when ΔT is small. From Eq (9), the $d\hat{w}/dt$ can be determined as follows:

$$\frac{d\hat{w}}{dt} = \frac{V_{\text{feedrate}}(\hat{w}_k)}{\sqrt{U'^{\mathrm{T}} G U'}} \tag{12}$$

From Eq (12), the $d^2\hat{w}/dt^2$ can be found as follows:

$$\frac{d^2\hat{w}}{dt^2} = \frac{\left(\sqrt{U'^{\mathrm{T}} G U'}\right)^3 \frac{\partial V_{\text{feedrate}}}{\partial \hat{w}} \frac{d\hat{w}}{dt} - \frac{\partial^2 (U'^{\mathrm{T}} G U')}{\partial \hat{w}^2} \bullet \frac{\partial (U'^{\mathrm{T}} G U')}{\partial \hat{w}} (V_{\text{feedrate}})^2}{\left(\sqrt{U'^{\mathrm{T}} G U'}\right)^4} \tag{13}$$

where the $\bullet$ represents the vector inner dot operation. By substituting Eqs (12) and (13) into Eq (11), we can find the new corresponding parameter $\hat{w}_{k+1}$ of the next reference point on the 3D curve $C_{xyz}(\hat{w})$ such that the curve speed satisfies the given feedrate $V_{\text{feedrate}}(\hat{w})$.

5. SURFACE-BASED NURBS PATH INTERPOLATION

As shown in Fig 6, during multi-axis NC machining the cutter is moving along CC paths with a series of pre-determined local inclination and tilt angles (λ,ω). Each set of inclination and tilt angle (λ,ω) is correspondent to a specific local coordinate system defined at each CC point at the time t [26, 27]. Sections 3 and 4 present the CC paths and the curve parametric increment for feedrate control. Using technique similar to Eq (5), the corresponding (λ,ω) can be determined for each curve parameter $\hat{w}$ at the time t.

However, the CC paths and the cutter local inclination and tilt angles (λ,ω) are not the machine tool trajectories. To guide the cutter to machine the part surface along the CC paths with such local inclination and tilt angle (λ,ω), the cutter needs to be positioned at the pivot point locations p_{pvt} with the corresponding spindle orientations (θ_B,θ_C), as shown in Fig 6.

As depicted in Fig 3, in this research the developed CAD/CAM/CNC architecture performs inverse kinematics in the interpolator of the machine tool control unit, rather than in the post-processors. Here we demonstrate the inverse kinematics for a spindle-tilt type 5-axis CNC machine tool as shown in Fig 6. For other types of machine tool configurations and details, readers can refer to any popular Robotics books such as [28].

The machine tool location and orientation can be determined by transforming the cutter representation from the cutter coordinate system into the local coordinate system (LCS), and then into the machine coordinate system (MCS) as follows:

$$\psi_{\mathrm{M,ctr}} = \begin{bmatrix} \psi_{\mathrm{M}\text{-}x} & \psi_{\mathrm{M}\text{-}y} & \psi_{\mathrm{M}\text{-}z} & 1 \end{bmatrix}^T = Matrix[\mathrm{MCS} \leftarrow \mathrm{LCS}]\, Matrix[\mathrm{LCS} \leftarrow \mathrm{cutter}](\lambda, \omega)\, \psi_{\mathrm{ctr}} \tag{14}$$

where ψ_{ctr} is the cutter representation in the cutter coordinate system (CCS). The origin of the ψ_{ctr} is defined at the cutter tip.

As shown in Fig 5, the cutter is held by the machine tool spindle. During NC machining, the spindle is being moved by referring to the pivot point p_{pvt} with spindle orientation (θ_B,θ_C). Thus, the spindle representation ψ_{spindle} can be transformed to MCS as follows:

$$\psi_{\mathrm{M,spindle}} = Matrix[\mathrm{MCS} \leftarrow \mathrm{spindle}]\, \psi_{\mathrm{spindle}} = \begin{bmatrix} 1 & 0 & 0 & x_{\mathrm{pivot}} \\ 0 & 1 & 0 & y_{\mathrm{pivot}} \\ 0 & 0 & 1 & z_{\mathrm{pivot}} \\ 0 & 0 & 0 & 1 \end{bmatrix}_{\mathrm{transMS}} \begin{bmatrix} \cos\theta_C & -\sin\theta_C & 0 & 0 \\ \sin\theta_C & \cos\theta_C & 0 & 0 \\ 0 & 0 & 1 & 0 \\ 0 & 0 & 0 & 1 \end{bmatrix}_{\mathrm{rot}\text{-}\theta_C} \begin{bmatrix} \cos\theta_B & 0 & \sin\theta_B & 0 \\ 0 & 1 & 0 & 0 \\ -\sin\theta_B & 0 & \cos\theta_B & 0 \\ 0 & 0 & 0 & 1 \end{bmatrix}_{\mathrm{rot}\text{-}\theta_B} \psi_{\mathrm{spindle}} \tag{15}$$

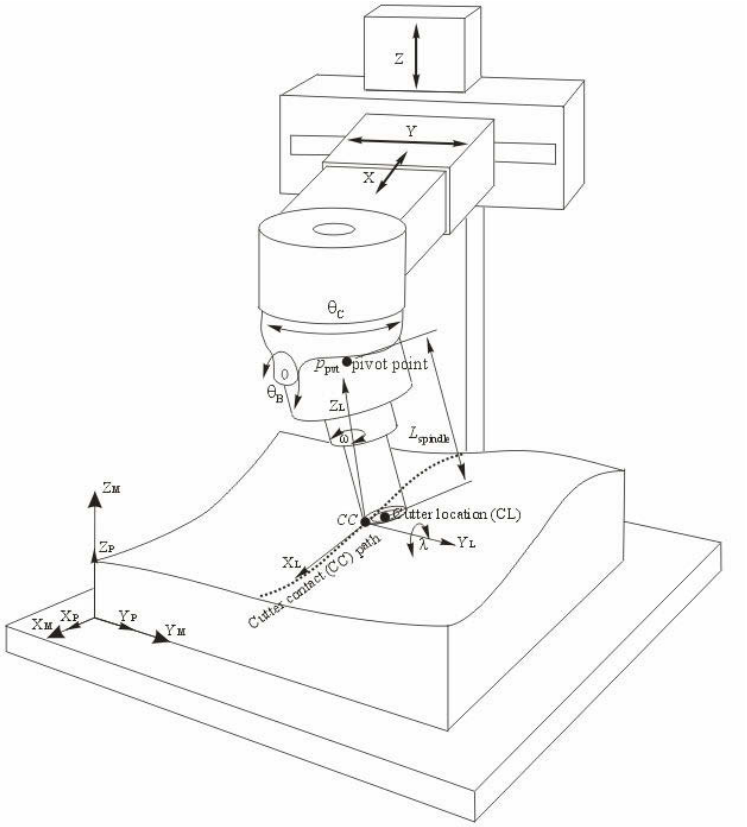

Fig. 5: Five-axis machine tool and part surface.

The origin of the spindle ψ_{spindle} is defined at the pivot point p_{pvt} of the spindle. In Eq (15), θ_B is the first spindle rotation angle, θ_C is the second spindle rotation angle, and (x_{pivot},y_{pivot},z_{pivot}) is the pivot point p_{pvt} location in the MCS, as shown in Fig 5. Since the cutter axis coincides with the spindle axis, the spindle rotational angles θ_B and θ_C can be solved by setting $\psi_{\mathrm{ctr}} = [0\ 0\ 1\ 0]^{\mathrm{T}}$ in Eq (14) and $\psi_{\mathrm{spindle}} = [0\ 0\ 1\ 0]^{\mathrm{T}}$ in Eq (15), then equalizing Eq (14) with Eq (15). θ_B and θ_C can be determined as follows:

$$\theta_B = \pm\cos^{-1}\left(\psi_{M\text{-}z}\right) \tag{16}$$

$$\theta_C = \cos^{-1}\left(\frac{\psi_{M\text{-}x}}{\sin\theta_B}\right), \text{ and } \theta_C = \sin^{-1}\left(\frac{\psi_{M\text{-}y}}{\sin\theta_B}\right) \tag{17}$$

Similarly, by setting $\psi_{spindle} = [0\ 0\ -L_{spindle}\ 1]^T$ in Eq (15) and $\psi_{ctr} = [0\ 0\ 0\ 1]^T$ in Eq (14), then equalizing Eq (14) with Eq (15), the pivot point location p_{pvt} can be solved as follows:

$$p_{pvt} = \begin{bmatrix} x_{pivot} \\ y_{pivot} \\ z_{pivot} \end{bmatrix} = \begin{bmatrix} \psi_{M\text{-}x} + L_{spindle}\cos\theta_C \sin\theta_B \\ \psi_{M\text{-}y} + L_{spindle}\sin\theta_C \sin\theta_B \\ \psi_{M\text{-}z} + L_{spindle}\cos\theta_B \end{bmatrix} \tag{18}$$

The combination of the pivot point location (x_{pivot}, y_{pivot}, z_{pivot}) and the spindle orientation (θ_B, θ_C) composes of the machine tool trajectory. To control the cutter to machine the part surface along the *CC* paths during NC machining, the machine tool reference pivot point p_{pvt} needs to be guided to the (x_{pivot}, y_{pivot}, z_{pivot}) of Eq (18) with the spindle orientation (θ_B, θ_C) of Eqs (16) and (17), as depicted in Fig 5.

The surface-based NURBS path interpolation derives the pivot point location p_{pvt} and the spindle orientation (θ_B, θ_C) from the *CC* paths on the part surface. Thus, the part geometry, the *CC* paths (in *u-v* domain), the cutter local inclination and tilt angles (λ,ω), and the feedrate are essential to implement the developed surface-based NURBS path interpolation for machine tool trajectory calculation.

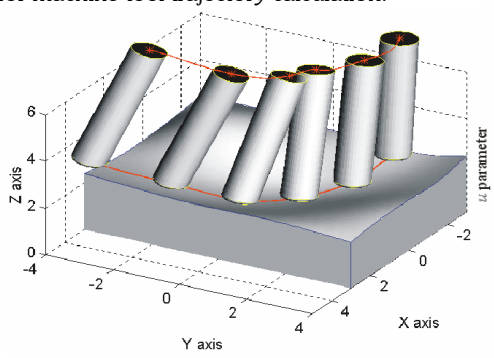

(a) Free-form 3D path on part surface

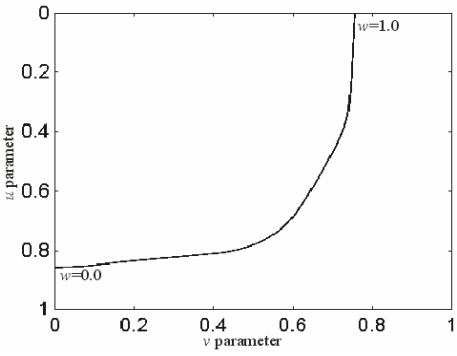

(b) Converted 2D (u,v) domain curve

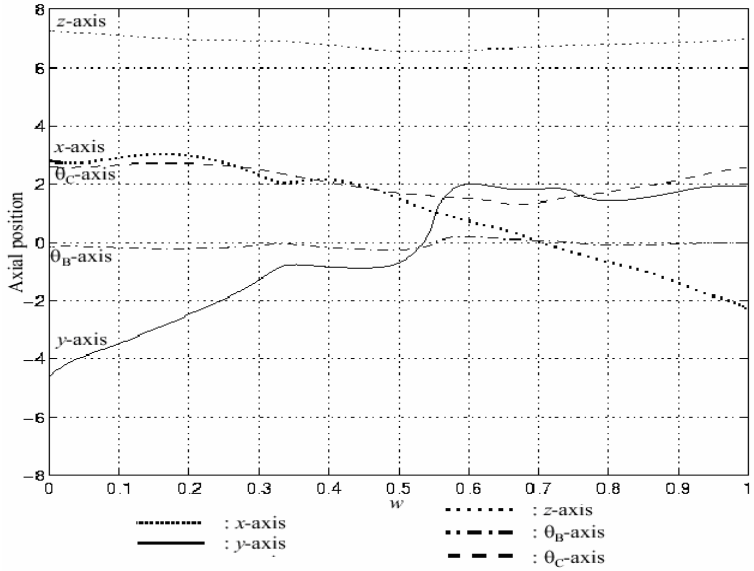

(c) Cutter speed and spindle rotation along different axes for example 5-axis tool path generation

Fig. 6: Example of 5-axis tool path along free-form CC path on sculptured surfaces.

6. COMPUTER IMPLEMENTATION AND EXAMPLES

The proposed method and techniques have been implemented on 2.66 GHz personal computers using C++ programming language at North Carolina State University. Fig 6(a) shows an example sculptured surface with an arbitrary NURBS CC (cutter contact) path on the part surface. The example 3D NURBS path is determined by maximizing the machining strip width and following the optimal cutting direction using the Machining Potential Field method discussed in our earlier works presented in [24, 29]. The sampling time ΔT of the CNC control unit is 0.005 seconds. A fillet-end cutter with radius r=0.5 units and corner radius r_{tc}=0.125 units and a ball-end cutter with radius r=0.5 units are used in the examples. The distance from the cutter tip to the pivot point is $L_{spindle}$=5.0 units.

Fig 6(b) shows the converted 2D u-v domain curve of the example 3D (X,Y,Z) NURBS CC path of Fig. 5(a). For instance, in Fig. 5(b), the λ, ω and f at the *CC* path point (u, v)=(0.82, 0.29) (where w=0.2) can be found as (λ, ω, f) = (10.62°, 4.05°, 11.0). The NC part program is then output to a spindle-tilt type 5-axis CNC machine tool with the developed surface-based NURBS interpolation. As shown in Fig 6(c), the presented surface-based NURBS path interpolation calculates the pivot point location and spindle orientation, and control the tool motion to machine the part surface along the arbitrary NURBS path.

Fig 7 shows a ball-end cutter that is machining a complicated part along the fillet between the shaft and the guard wall. Due to the complex geometry, the fillet is impossible to be machined with fixed cutter axis or any constant inclination and tilt angles. Instead, interactively calculating the local inclination and tilt angles (λ,ω) and verifying gouge and interference in CAM systems are necessary before NC machining. Fortunately, unlike the surface interpolations by which users can not control the cutter orientation, the developed surface-based NURBS path interpolation can take the well-planned tool paths with the safe cutter inclination and tilt angles (λ,ω) from CAM systems. Cutter gouge and tool interference can be fully avoided during NC machining.

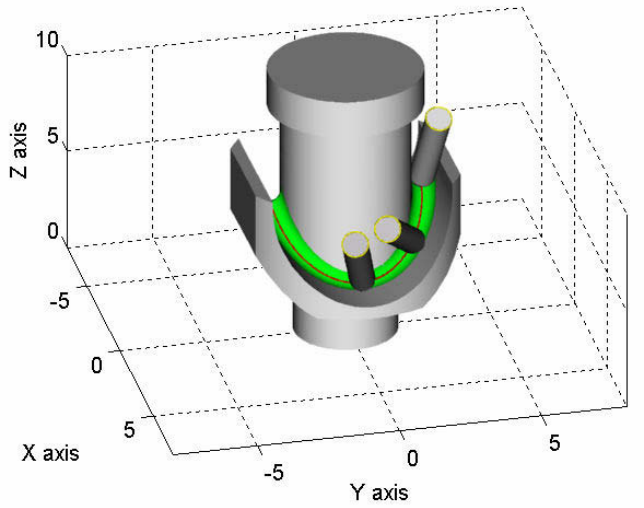

Fig. 7: NURBS path interpolation for 5-axis machining of example surface between the shaft and the guard wall.

Fig 8 shows the comparison of the machined surface errors along the example tool path by using the following different methods: the linear, the curve and the surface-based NURBS path interpolation methods. The CC path in this example is approximated by using 11 control points. The machining errors are determined by the computer simulation with G-buffer methods. Fig 8(a) shows the machined surface error $-0.1840 \le \tau^{L} \le 0.0271$ along the CC path by the linear interpolation. Fig 8(b) shows the machined surface error $-0.1060 \le \tau^{C} \le 0.0425$ along the CC path by the curve interpolation. Fig 8(c) shows the machined surface error $-0.001 \le \tau^{S} \le 0.001$ along the CC path by the developed surface-based NURBS path interpolation. Note that the scale of the error axis (horizontal axis) in Fig 8(c) is different from that in Figs 8(a) and 8(b).

By observing Fig 8, the developed surface-based NURBS path interpolation generates machine tool trajectory with much smaller interpolation errors along the CC paths (i.e., $|\tau^{L}| > |\tau^{C}| > |\tau^{S}|$). This is consistent with our previous observation that, by using the proposed surface-based NURBS path interpolation, the CC paths can be easily defined on part surface and then mapped into the u-v domain for 5-axis tool path generation. The pivot point location and the spindle orientation (θ_B,θ_C) are directly derived from the 3D CC paths on the part surface. Thus, the cutter always

touches the part surface along the tool paths. The chordal-swept deviation errors can be reduced. Compare with the linear interpolation method (Fig 8(a)) and the curve interpolation method (Fig 8(b)), the developed interpolation method can generate tool motions with higher accuracy ($|\tau^L| > |\tau^C| > |\tau^S|$) and reduce the machining errors for multi-axis NC machining.

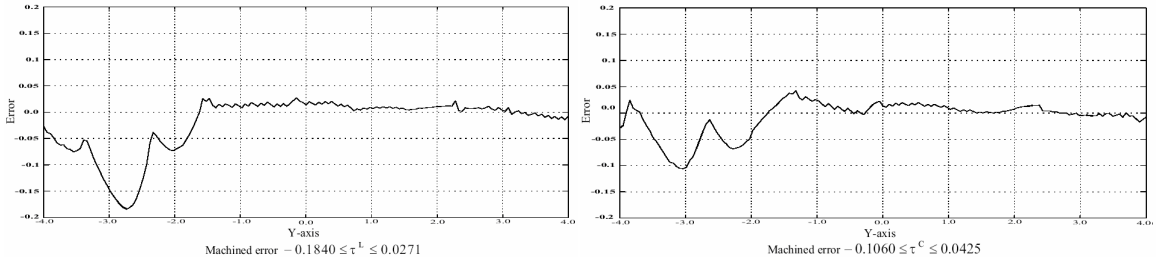

(a) by linear interpolation (b) by curve interpolation

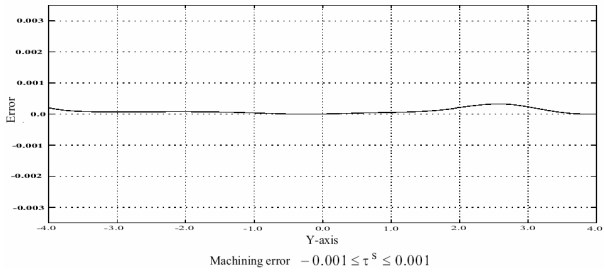

(c) by proposed surface-based NURBS path interpolation

Fig. 8: Comparison of free-form tool path interpolation errors by different methods.

8. CONCLUSIONS

This paper presents a new surface-based NURBS path interpolation for multi-axis NC machining. The developed surface-based NURBS path interpolation directly takes the cutter contact (CC) points on the part surface as the reference points to control the multi-axis machine tool movements. The positioning errors of the chordal deviation and the swept deviation of the current linear and curve interpolations can be reduced. In addition, inverse kinematics is performed by the developed surface-based NURBS path interpolator during NC machining, NC part programs can be independent from the machine tool configurations. Analytic formulations of multi-axis tool motions and NURBS path interpolation have been presented for machine tool control in complex surface machining. Comparing to other existing methods, the developed NURBS path interpolation method can obtain better multi-axis tool trajectory with higher interpolation accuracy. The presented techniques can be used in the CAD/CAM systems and the NC controllers for 5-axis high speed machining of sculptured surfaces.

9. ACKNOWLEDGEMENT

This work was partially supported by the National Science Foundation (NSF) Grant (DMI-0300297 and DMI-0553310) and the Army Research Office (Grant #W911NF-04-D-0003) to North Carolina State University. Their support is greatly appreciated.

10. REFERENCES

[1] Yang, D. C. H.; Kong, T.: Parametric interpolator versus linear interpolator for precision CNC machining, Computer-Aided Design, 26(3), 1994, 225-234.

[2] Ren, Y.; Lee, Y.-S.: Time-Based Parameter Path Interpolation for High Speed Machining, Proceedings of 2006 High Speed Machining Conference, Metz, France, March 14-16, 2, 2006, 577-586.

[3] Filip, E.; Magedson, R.; Markot, R.: Surface algorithms using bounds on derivatives, Computer Aided Geometric Design, 3, 1986, 295-311.

[4] Zhang, Q. G.; Greenway, R. B.: Development and implementation of a NURBS curve motion interpolator, Robotics and Computer-Integrated Manufacturing, 14, 1998, 27-36.

[5] Koren, Y.: Control of Machine Tools, Journal of Manufacturing Science and Engineering, 119, 1997, 749-755.

[6] Liang, H.; Hong, H.; Svoboda, J.: A combined 3D linear and circular interpolation technique for multi-axis CNC machining, Journal of Manufacturing Science and Engineering, 124(2), 2002, 305-312.
[7] Kloypayan, J.; Lee, Y.-S.: Material Engagement Analysis of Different Endmills for Adaptive Feedrate Control in Milling Processes, Computers in Industry, 47(1), 2002, 55-76.
[8] Li, S. X.; Jerard, R. B.: 5-axis machining of sculptured surfaces with a flat-end cutter, Computer-Aided Design, 26(3), 1996, 165-178.
[9] Sarma, R.; Rao, A.: Discretizers and interpolators for five-axis CNC machines, Proceedings of the ASME Dynamic Systems and Control Dviision, ASME, DSC-Vol.64, 1998, 447-454.
[10] Suh, S.-H.; Lee, K.-S.: Avoidance tool interference in four-axis NC machining of rotationally free surfaces, IEEE Transactions on Robotics and Automation, 8(6), 1992, 718-728.
[11] Taylor, R. H.: Planning and execution of straight line manipulator trajectories, IBM Journal of Research and Development, 23(4), 1979, 424-436.
[12] Takeuchi, Y.; Watanabe, T.: Generation of 5-axis control collision-free path and post-processing for NC data, Annals of the CIRP, 41(1), 1992, 539-542.
[13] Shpitalni, M.; Koren, Y.; Lo, C. C.: Realtime curve interpolators, Computer-Aided Design, 26(11), 1994, 832-838.
[14] Chou, J.-J.; Yang, D. C. H.: On the generation of coordinated motion of five-axis CNC/CMM machines, Journal of Engineering for Industry, 114(1), 1992, 15-22.
[15] Farouki, R. T.; Shah, S.: Real-time CNC interpolators for Pythagorean-hodograph curves, Computer Aided Geometric Design, 13, 1996, 583-600.
[16] Lin, R.-S.: Real-Time Surface Interpolators for Multi-Axis CNC Machine Tools, Ph.D. Dissertation, The University of Michigan, 1994.
[17] Omirou, S. L.: Space curve interpolation for CNC machines, Journal of Materials Processing Technology, 141(3), 2003, 343-350.
[18] Kiritsis, D.: High precision interpolation algorithm for 3D parametric curve generation, Computer-Aided Design, 26(11), 1994, 850-856.
[19] Lin, R.-S.; Koren, Y.: Real-time five-axis interpolator for machining ruled surfaces, Proceedings of ASME Dynamic Systems and Control, ASME, 55(2), 1994, 951-960.
[20] Cheng, K.; Tang, S.-D.: NURBS-based multi-axis tool-path for high speed machining, Proceedings of 1999 ASME Design Engineering Technical Conferences, Las Vegas, ASME, 1999, DETC99/CIE-9111.
[21] Arnone, M.: High Performance Machining, Hanser Gardner Publications, 1998.
[22] Farin, G. E.: Curves and Surfaces for CAGD, Morgan-Kaufmann, 5th Edition, 2001.
[23] Piegl, L.; Tiller, W.: The NURBS Book, 2nd Edition, Springer-Verlag Berlin Heidelberg, Germany, 1997.
[24] Chiou, C.-J.; Lee, Y.-S.: Machining potential field approach to tool path generation for multi-axis sculptured surface machining, Computer-Aided Design, 34(5), 2002, 357-371.
[25] Faux, I. D.; Pratt, M. J.: Computational Geometry for Design and manufacture, Ellis Horwood Limited, 1983.
[26] Chiou, C.-J.; Lee, Y.-S.: A shape-generating approach for multi-axis machining G-buffer models, Computer-Aided Design, 31(12), 1999, 761-776.
[27] Lee, Y.-S.: Admissible tool orientation control of gouging avoidance for 5-axis complex surface machining, Computer-Aided Design, 29(7), 1997, 507-521.
[28] Craig, J.: Introduction to Robotics: Mechanics and Control, Prentice Hall, 2005.
[29] Chiou, J.C-J.; Lee, Y.-S.: Multi-Axis Sculptured Surface Machining, International Journal of Manufacturing Research, 1(2), 2007, 213-247.